

Author's Response to Reviewers' comments

Associate Editor

The same two anonymous reviewers have read the resubmitted version of your manuscript, along with the response to reviewers that you provided. They reach differing conclusions (reject vs minor revisions). It is my opinion that many of the points that reviewer 1 raises, are fair. Indeed there appears to be insufficient consideration of the concerns that this reviewer raised based on the first version of the paper. More changes are clearly required. Reviewer 2, although less critical, agrees at least on one point: that one of your most important formulae has wrong units. To my mind, this means that adaptation is required, and that model reruns with reconsideration of results are necessary. I translate this into a request for resubmission after major revisions.

Should you decide to resubmit an improved manuscript, please make sure to provide a detailed response that reflects the importance of reviewer 1's concerns. *We would like to thank the Editor, Associate Editor and two referees for their continued efforts in this process.*

Reviewer #1

1) In my previous review I commented that the fact that a model with both fluvial and diffusive processes works better than one with just diffusive or just fluvial processes is not a significant conclusion. In their response the authors state that this is not a conclusion of their study (i.e., "the conclusion of this study is NOT that both transport mechanisms are in play..."). In fact, the text of the paper makes clear that this is major conclusion of their paper. Their conclusion section states "Only by simulating both fluvial and diffusive transport mechanisms can the model correctly simulate the observed soil distribution."

We did not intend to make this a major conclusion. However, it is an interesting demonstration of how both processes effect soilscape evolution under these unique conditions. Hancock et al (2002) demonstrated that the inclusion of diffusion was extremely important for correctly simulating landscape evolution. We see this statement as part of the conclusion not THE conclusion and it is stated in the context of the new insights of this study: "Only when both fluvial and diffusive sediment transport mechanisms were modeled, a reasonable correspondence was achieved. While soilscares are generally thought off as resulting from both transport mechanisms, this and previous studies demonstrates that fluvial-diffusion coupling is more pronounced in aeolian dominated soilscape."

However, I accept the fact that the authors are also examining how the relative importance of diffusive versus fluvial processes varies with topographic position. *Thank you.*

However, the authors do not provide any reason why the addition of mass in the form of aeolian deposition would fundamentally alter the relative importance of

fluvial versus diffusive processes as a function of topographic position, which was considered in Cohen et al. (2015) for what the authors call "bedrock (normal) landscapes".

We respectfully disagree. Please see these two paragraphs in the introduction (and a whole separate paper on this topic – Cohen et al., 2015):

"From a soilscape evolution point of view, aeolian dominated soilscales differ from bedrock-weathering dominated soilscales in several ways. In bedrock-weathering systems in situ weathering rates decrease exponentially with soil depth (Gilbert, 1877; Ahnert, 1977), thus regulating soil production as a function of regolith thickness (Heimsath et al., 1997). Weathering of regolith and soil leads to vertical particle size distribution with finer particles closer to the surface as a function of the soil and regolith age, namely time exposed to weathering (Yoo and Mudd 2008). At the surface, armouring can develop by size-selective entrainment (Kim and Ivanov, 2014) or vegetation shielding, which limits sediment transport by overland flow (Willgoose and Sharmeen, 2006). Given sufficient time and in the absence of vertical mixing due to pedoturbation, these processes - depth dependent weathering, vertical self-organization and surface armouring - will stabilize the soilscape leading to steady-state or dynamic equilibrium conditions (Cohen et al., 2013 & 2015). In aeolian dominated landscapes these controls on soil production and transport are largely ineffective as: (1) much of the soil is transported to the system as airborne sediments, i.e., no depth dependency; and (2) fine and highly erodible material is continuously deposited on top of older surface soils which limits the potential for surface armouring and vertical self-organization.

The differences between aeolian and bedrock-weathering dominated soilscales lead us to conclude that traditional (i.e. bedrock weathering originated) soilscape evolution analysis is inappropriate for investigating the history of the aforementioned loess soilscales. In Cohen et al. (2015) we developed a soilscape evolution model (mARM5D) to study the differences and interactions between aeolian and bedrock weathering soil production on a synthetic 1D hillslope. In that paper we have found that bedrock weathering dominated soilscales are considerably more stable and showed much lower spatial (aerial) variability in soil depth and particle size distribution (PSD). We proposed that aeolian-dominated landscapes are more responsive to environmental changes (e.g., climatic and anthropogenic) compared with bedrock-weathering landscapes. "

Instead, they simply modify the values of key parameters (n_4 and β especially) without calibration to data, then conclude that aeolian soilscales lead to a completely different ratio of fluvial to diffusive processes as a function of topographic position than bedrock landscapes. I would be completely in support of this result if there was actual evidence presented that n_4 and β should be 0.1 for this field site or any other aeolian soilscape, but there is simply no data presented to demonstrate that these are the correct values. I continue to believe that any difference between the results of this paper and that of Cohen et al. (2015) for bedrock landscapes results not from the fact that one is a "bedrock (normal)" landscape and the other an "aeolian soilscape" but rather that this study has chosen

very different and ad hoc values for n_4 and β that have no justification and no clear connection to this or any other aeolian-dominated landscape.

We respectfully disagree with the above comment. Cohen et al. (2015) "*The effects of sediment - transport, **weathering and aeolian** mechanisms on soil evolution*"

explored the difference between bedrock weathering and aeolian dominated soils. In that paper we used $n_4 = 1$ and $\beta = 1$ as is commonly used. In this current manuscript we present a conceptual study of a specific case study – semi-arid, aeolian dominated, soil-depleted and high-gradient soilscape- focusing on differences between fluvial and diffusive transport mechanisms on this type of soilscape. We are NOT investigating the differences between aeolian and bedload dominated soils in this paper! This comment most likely stems from the section in the discussion that focuses on the differences between aeolian and bedrock soils. We have revised it to clarify the point that the two studies cannot be directly compared.

Regarding the values of these two coefficients- in response to the reviewer and associate editor comments, we have conducted a new analysis for a 1D hillslope in our field site (near transects we discuss in the manuscript). To isolate the effects of n_4 and β values on the model results we ran these 1D simulations without the temporal change scenario. Simulating without the change scenario changes the overall transport rates and the soilscape evolution and is therefore not readily comparable to the landscape simulations presented in the manuscript. This allows us, however, to adjust the transport rating (due to differences in the β and n_4 coefficients) to more clearly isolate the effects of β and n_4 . We compared the following simulations:

n_4 and $\beta = 1$

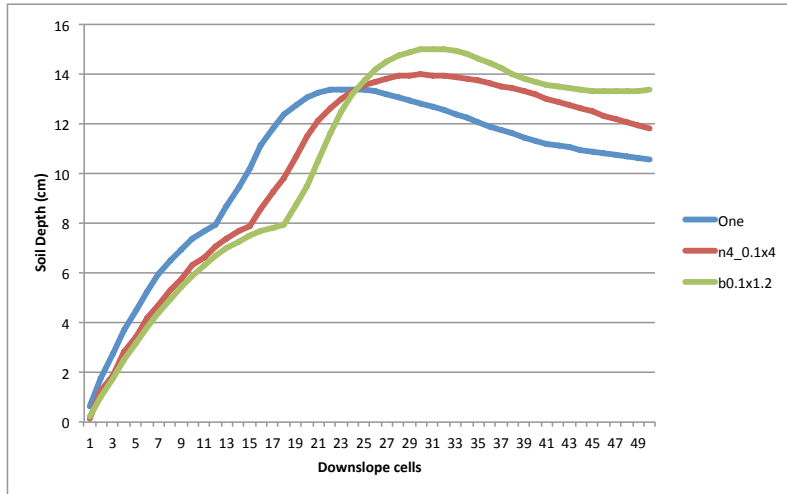
$n_4 = 0.1$ and $\beta = 1$

$n_4 = 1$ and $\beta = 0.1$

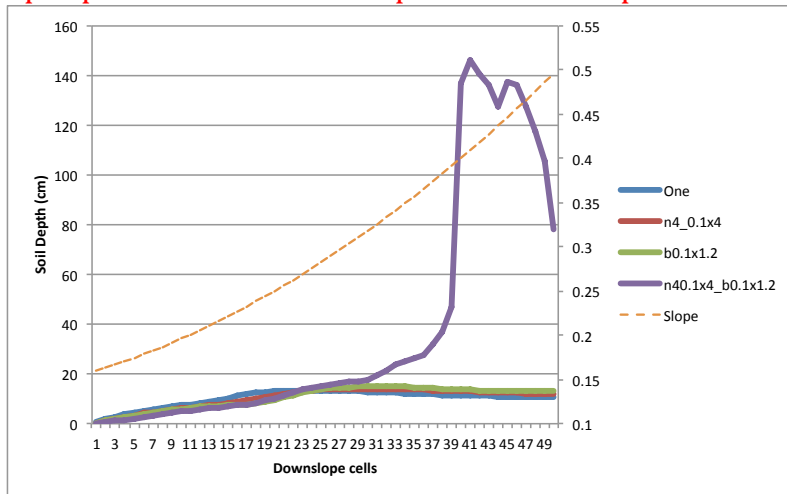
$n_4 = 0.1$ and $\beta = 0.1$

Since the change in β and n_4 affects the fluvial and diffusive transport rates ($=0.1$ will reduce the rate), we first had to adjust these rates so the resulting soil distribution will be, as much as possible, due to differences in coefficient value and not due to differences in transport rate. We did that by finding (by calibration) the rate adjustment (increase) factor resulting in total soil depth that is similar to a simulation in which both coefficients equal 1. We found that a factor of 4 is needed for when $n_4=0.1$ and a factor of 1.2 is needed for when $\beta=0.1$.

The results show that changing only one of the coefficients (n_4 or β) to 0.1 resulted in relatively little difference in soil distribution down this concave hillslope:



When both n_4 and β equal 0.1 the soil distribution was very similar at the upslope section of the hillslope but much deeper soil at the downslope section:



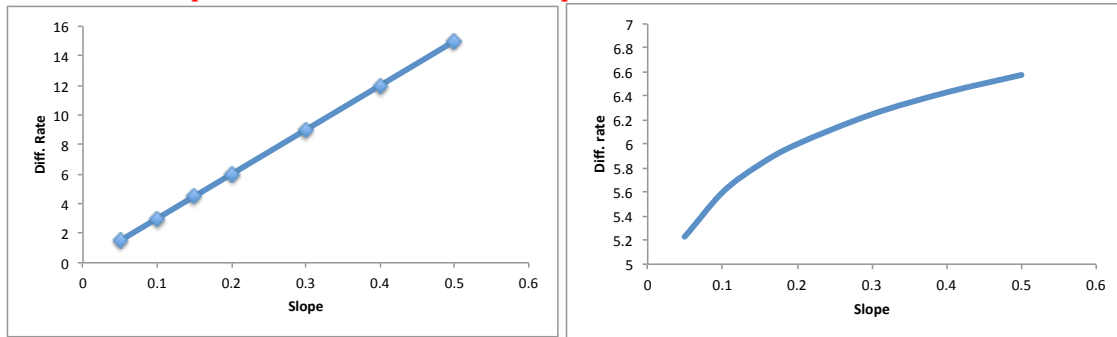
This soil distribution shape is quite common in our field site, a hump of deep soil driven by the balance between slope and area values (high slope mainly increase diffusion while high area increase fluvial transport). It could be argued that similar distribution could be achieved by adjusting the transport rates with n_4 and β equal to 1. Our analysis showed that this was not the case given the high concave down slopes of our field site.

This analysis is further expended in a separate study which is forthcoming. It is too complex and may be incomplete to expand in this current manuscript.

In their rebuttal the authors present two figures of soil diffusivity versus slope that purport to show a calibration, but there is no data in these figures. They appear to be simply graphs of S^1 and $S^{0.1}$.

Yes, we agree that they are and we should have explained that plots better. The intention was to show the effect of β on diffusion rate for a range of slope values. As can be seen, a $\beta=0.1$ (right plot) reduces the range of change down the hillslope.

We suggest that this is why a $\beta=0.1$ is needed for this site given its steep concave-down shape (increasing slope gradient downslope). This assertion was added in the last manuscript revision and now developed even further in the 2nd revision.



A more minor but related issue is that I don't think that bedrock (normal) landscapes and aeolian soils are fundamentally different kinds of landforms. They exist on a continuum, since soils everywhere in the world contain some fraction of material derived from in situ weathering and some from aeolian deposition.

Yes, this is correct -but what about the extremes where aeolian deposition has considerable influence on soil depth and properties – that is the extreme end of the soilscape spectrum? There are many aeolian-dominated soils which – as we described in the introduction and explored in our last paper – are potentially much different in some aspects. For example our analysis suggests that aeolian-dominated soils are more susceptible to environmental changes. Ultimately, that is really what we are exploring here.

This was my point when I recommended to the authors that they obtain some data (using immobile element ratios or similar geochemical techniques) on the relative fraction of the soil derived from aeolian input versus in situ weathering. The authors countered that they don't need data because the aeolian-dominated nature is clear from "walking the site." I don't know what this means.

We may have had a misinterpretation here. We said that this region was studied extensively for many years and it is well established that the soil has a strong aeolian input. The relevant literature is cited in the manuscript.

2) I agree that some type of power-law relationship with depth and slope is correct for fluvial transport, so I am not going to harp on the fact that there is little clarity in how the authors have modified Engelund and Hansen (1967) to arrive at their eqn. (1). The fact remains that, if the reader looks at p. 42 of Engelund and Hansen (actually p. 41) there is an expression for the Shields stress as a function of the mean dune height and other parameters. How these equations relate to equation (1) of Cohen et al. remains unclear. Referring me to TOPOG or some other model does not answer the question of how one goes, step by step, from one or more of Engelund and Hansen's equations to eqn. (1) of Cohen et al., which is what I think readers need (in an appendix would be fine, if the authors consider this to be ancillary).

As we acknowledged in our response that directly referencing Eq 1 to Engelund and Hansen (1967) was not the best approach even though it is the equation origin. The equation was adopted from the TOPOG model and that was clearly referenced in the last revision. We have now also added a reference to Merritt et al (2003) review paper where they outline this link. TOPOG is a well used and vetted model and we don't think we need to retrace their adaptation step-by-step.

3) Yair and Kossovsky (2012) may provide a basis for using a value of n_4 that is lower than 1. However, the authors have provided no justification for the specific value they used (0.1) either in the paper or in their rebuttal. This value still seems to be pulled from thin air. Why not 0.3 or 0.5? This is a major issue, since the value of n_4 directly controls the strength of the fluvial term in the model, and its variation with topographic position.

We tested a range of values and found 0.1 to better match observed soil distribution. We agree that this is an intriguing result that merit further investigation. This is now discussed in the manuscript.

4) I am very disturbed by the author's statement that "Diffusion absolutely involved routing, how else does the model transport the sediment down the slope?" This seems to indicate that the authors do not know how to model diffusion. Diffusion is the divergence of a flux. The divergence of a flux is defined as the derivative of the x component of the flux in the x direction plus the derivative of the y component of the flux in the y direction. Flow routing such as D8 do not appear anywhere in the definition of divergence and SHOULD NOT be used for diffusion on hillslopes. There is certainly no reason why flow routing methods are REQUIRED to model diffusion. The fact that D8 is being incorrectly used leads directly to the unrealistic "striping" seen in the results. Obviously, any model result that shows large variations in model results along 45 or 90 degrees is a model artifact that needs to be minimized. I don't see any of this kind of striping in other aeolian soilscape models that have been used in the literature to model soil depth or aeolian soil fraction (which are not referenced). This is a major issue that simply must be fixed.

We have extended the description of these features and now provide a more concise explanation.

Regarding the use of D8 for diffusion transport - the flux form for diffusion is $q_s = DS = -D \, dz/dx$. This is fundamentally how diffusion is defined based on a gradient of the constituent being diffused. The 2nd order finite difference term commonly used is subsequently defined based on mass continuity equations (the divergence term mentioned by the reviewer) using this flux equation so that $dz/dt = -D \, (dz^2/dx^2 + dz^2/dy^2)$ and the finite difference approximation typically discussed is derived directly from this. Mathematically these two forms for diffusion are equivalent. The approximations that is used in mARM5D uses the flux form and follows the approach used in the first of the landform evolution models SIBERIA (Willgoose et al 1991). Essentially the D8 is used to determine the flux direction, and the amount of flux per time step is determined by the flux form of the diffusion equation. SIBERIA originally used the finite difference form of the equation but subsequent testing showed the flux form gave very similar results while being

MUCH easier to implement for (1) irregular boundaries and (2) variable spaced grids.

However, the reviewer is right ... doing flow routing is not required ... it is included and used in conjunction with other processes (e.g. erosion) and more realistic problems with irregular boundaries and variably spaced grids or TINS.

5) In my review I noted that D8 cannot be used for hillslopes, where the flow of water and fluvial sediment is divergent (D8 assumes strong convergence everywhere). The authors counter that they have developed a fast model and so any inaccuracies should be acceptable in the name of speed. I disagree. I think the model needs to be accurate first. Again, this is a major issue that must be addressed.

Yes, we agree. This was poorly worded. Each drainage direction algorithm has its strengths and weaknesses. To the best of our knowledge most models use D8 routing (some even use D4, i.e. CAESAR) as it is a much more efficient algorithm. Yes, we could start to employ different routing algorithms but this would greatly complicate an already complex modeling study. In fact we do not know of any model that differentiates between drainage direction based on convergence/divergence. However we see this as an important next step and added this comment to the manuscript. We also recognize that efficiency is important to these kind of studies. We argue that the while a more flexible algorithm may help resolve some of the problems we observed in our simulations (which are discussed in the manuscript) the overall insight from this study would be the same. We acknowledged that this is a needed improvement in the model (and other models).

6) As with the value of n_4 , no calibration is performed to show that $\beta = 0.1$ for this field site, either in the paper or in the rebuttal. To do this calibration, the authors would need data. There is no data in the two figures provided in the rebuttal, which appear to simply be plots of S^1 and $S^{0.1}$. The authors may be correct that $\beta = 0.1$ is an interesting result, but the authors need to show the readers (via some type of least-squares or other fit to DATA) why $\beta = 0.1$ at this location.

See response to comments 1 and 2.

7) Equation (4) continues to have a units problem. In their rebuttal the authors state that equation (4) does not have a time step but I am looking at eqn. (4) right now and the last term is “delta t”.

You are correct – we thought you were referring to equation 3.

Since diffusivity is always L^2/T and the only other term with units is delta t then D must have units of L^2 . However, the reported units are L/T . The authors may think that “In practice it makes not difference” but I think it will matter to readers trying to replicate their work. The authors have indicated that their diffusivity has units of L (no units were reported in the paper so I was guessing that diffusivity had units of L^2/T , which is always the proper unit of diffusivity), but this still leads to a units

problem since if I use units of L for diffusivity, then according to eqn. (4) D should have units of L^2/T , not L/T .

The model calculates the **proportion** of each layer that is displaced due to diffusion (L relative to L of the cell). That proportion decrease exponentially down the soil profile (Eq. 3) in proportion to the surface diffusion rate (eq. 4). In effect the PSD vector for each layer in each grid-cell is deducted by the multiplication of the PSD vector by the proportion of the layer that has been displaced (calculated by dividing the surface diffusion by cell size) plus a temporal adjustment parameter. We have simplified the description of this algorithm as it can be confusing without understanding the model's unique architecture (which is shortly describe at the start of the section with references to previous papers). We have revised the diffusion description sub-section to clarify this point. D_s is in units of m by multiplying D_0 (m/y) by dt . The actual change to soil is now shown in eq 5. D_s is divided by a grid cell length (m) to calculate a unitless proportion of sediment transported from a grid cell.

8) I am not going to comment on the author's response to my concerns about the weathering portion of their model, since I don't find it acceptable for the authors to refer me to older papers and send me code rather than simply answering my question.

We apologize, as there is some misunderstanding here. We had presented over a page of response just for the 1st reviewer's comments (see box below) on this issue:

When I tracked down Minasny and McBratney (2006) I found a rather different equation (their equation (4)). Equation (5) is dimensionally incorrect. It is wrong to have the steady state weathering rate appear inside the exponential – the argument of any exponential should be unitless. The equation was indeed (as stated) modified, the P_0 parameter was moved to allow for an above-zero watering rate at the surface while depth rates down the soil profile asymptote to zero. Cohen et al. (2010) focused on the model weathering equations and algorithm. We can see how the description of the model weathering calculations is confusing and misrepresentative. This stems, again, from our attempt to simplify a complex algorithm into one equation with time-varying parameter. The full algorithm includes compiling a transition matrix which control the transition of PSD in each particle size class to smaller class(s) in each soil-profile layer. The algorithm was described at length in Cohen et al. (2009 and 2010). The depth-varying weathering rate equation in the model (see the actual model FORTRAN function below) is not directly used to calculate weathering rate, rather the relative (normalized) change in weathering down the profile. As part of the revised model description we removed the section describing the weathering calculations as it does not include parameters that are modified in the simulation scenarios we analyzed in this paper.

```
#####  
! A function to calculate the decline in weathering rate as a function of depth  
! It return the WeatheringAlpha which is different for every layer
```

```

! The exponential function is taken from Minasny & McBratney (2006)
! de/dt=Po{Exp(-k1h)-Exp(-k2h)}+Pa ;
! Their original values are: Po-potential WR=0.25; k1=4; k2=6; Pa- steady state WR=0.005
! The function was changed in version 4.5.1 to account to close to zero weathering in
lower layers
#####
REAL*8 Function DepthWeatheringAlpha(WeatherAlpha,i,LayerDepth)
IMPLICIT NONE
Integer i
Real*8 WeatherAlpha, LayerDepth, Ratio, Depth
If (i==1) Then
Depth=0.5
Else
Depth=(i-1)*LayerDepth-(LayerDepth/2)
End If
Depth=Depth/100 !convert to meters
Ratio=(0.25*((EXP(-4*Depth+0.02))-(EXP(-6*Depth))+0))/0.04 !We divide by 0.04 to
normalize it
DepthWeatheringAlpha = WeatherAlpha*Ratio
Return
End Function DepthWeatheringAlpha

```

Why are delta_1 and delta_2 equal to 4 and 6? What are the units? If they are meters these are very large values (i.e. they imply that weathering rates fall off by a factor of e only once the soil is at least 4 m thick. This is a very thick soil). Following on the comment above, the model algorithm uses the Minasny and McBratney (2006) equation to get the relative change in weathering rate down the soil profile. These variables therefor control the shape rather than the actual weathering rate. Their values were based on Minasny and McBratney (2006) to maintain the relative change (i.e. shape of the hump function) and so in reality they are unitless.

9) I don't see how "walking the site" allows one to conclude that the fine grained component of the soil cannot be from weathering of bedrock. Again, data is needed. Yes, this is a poor choice of words. Aeolian deposition rates and soil formations were well studied in this region. References are provided in the manuscript and the aeolian rate was based on these. There is simply no need to go into further geochemical complexity and we consider the request to be unreasonable. The bedrock is limestone which is well known for low soil production rates – we made a simple assumption (which is clearly stated in the manuscript) that weathering rate is an order of magnitude lower than aeolian deposition (at baseline levels).

10) I asked for a table of parameters. The authors refer me to the last 4 papers on this model. Including a table is a very simple request and I am disappointed that the authors refuse to do even that much to assist the reader. The key parameters (with their symbology) are outlined in the methodology and again in Table 1.

I can see how the authors might view my review as an attack on their paper. However, I am really trying to help them meet common standards for accuracy and transparency.

We very much appreciate the comments. Thanks!

Reviewer #2

The authors have addressed all of the reviewers' comments. However the humped equation should be corrected, so that the units are correct:

The equation as presented in Minasny & Mcratney (2006)

$$de/dt = P_0 * (\exp(-k_1*h) - \exp(-k_2*h)) + P_a$$

where P_0 is the potential weathering rate (m/y), P_a weathering rate at steady-state and k_1 and k_2 are rate constants (units $1/m$).

The current formulation does not yield a correct unit:

$$Wl = P_0 \exp(-\delta_1 h_1 + P_a) - \exp(-\delta_1 h_1)]$$

The equation was modified into a normalized (unitless) change in weathering rate relative to surface weathering rate. The P_0 parameter was moved to allow for an above-zero watering rate at the surface while depth rates down the soil profile asymptote to zero. Cohen et al. (2010) focused on the model weathering equations and algorithm. We can see how the description of the model weathering calculations is confusing and misrepresentative out of the context of the full model algorithm. This stems, again, from our attempt to simplify a complex algorithm into one equation with time-varying parameter. The full algorithm includes compiling a transition matrix which control the transition of PSD in each particle size class to smaller class(s) in each soil-profile layer. The algorithm was described at length in Cohen et al. (2009 and 2010). The depth-varying weathering rate equation in the model is not directly used to calculate weathering rate, rather the relative (normalized) change in weathering down the profile. As part of the revised model description we removed the section describing the weathering calculations as it does not include parameters that are modified in the simulation scenarios we analyzed in this paper.

Soilscape evolution of aeolian-dominated hillslopes during the Holocene: investigation of sediment transport mechanisms and climatic-anthropogenic drivers

Sagy Cohen^{1,2*}, Tal Svoray², Shai Sela², Greg Hancock³ and Garry Willgoose⁴

¹ Department of Geography, University of Alabama, Box 870322, Tuscaloosa, Alabama 35487, USA.

² Department of Geography and Environmental Development, Ben-Gurion University of the Negev, Israel.

³ School of Engineering, The University of Newcastle, Callaghan, New South Wales 2308, Australia

⁴ School of Environmental and Life Sciences, The University of Newcastle, Callaghan, New South Wales 2308, Australia

* Corresponding author:

Email: sagy.cohen@ua.edu; Phone: 1-205-348-5860; Fax: 1-205-348-2278

Keywords: Soilscape, Pedogenesis, Sediment Transport, Modeling, Aeolian, Loess.

Submitted to: Earth Surface Dynamics

Abstract

Here we study the soilscape (soil-landscape) evolution of a field-site at the semiarid zone of Israel. This region, like similar regions around the world, was subject to intensive loess accumulation during the Pleistocene and early Holocene. Today, hillslopes in this region are dominated by exposed bedrock with deep loess depositions in the valleys and floodplains. The drivers and mechanism that led to this soilscape are unclear. Within this context, we use a soilscape evolution model (mARM5D) to study the potential mechanisms that led to this soilscape. We focus on advancing our conceptual understanding of the processes at the core of this soilscape evolution by studying the effects of fluvial and diffusive sediment transport mechanisms, and the potential effects of climatic and anthropogenic drivers. Our results show that in our field site, dominated by aeolian soil development, hillslope fluvial sediment transport e.g. surface wash and gullies, lead to downslope thinning in soil while diffusive transport e.g. soil creep lead to deeper and more localized soil features at the lower sections of the hillslopes. The results suggest that, in this semiarid, aeolian-dominated and soil depleted landscape, the top section of the hillslopes is dominated by diffusive transport and the bottom by fluvial transport. Temporal variability in environmental drivers had a considerable effect on soilscape evolution. Short but intensive changes during the late Holocene, imitating anthropogenic landuse alterations, rapidly changed the site's soil distribution. This leads us to assume that this region's soil depleted hillslopes are, at least in part, the result of anthropogenic drivers.

1. Introduction

Southern Israel, similar to other regions around the world, was subject to intensive loess accumulation during the Pleistocene and early Holocene. Hillslopes in this region are currently dominated by exposed bedrock with deep loess deposits in the valleys. The drivers and timing of the soilscape evolution that led to this soilscape are debatable. Studies in southern Europe and in the northern parts of the Middle East have found that anthropogenic activities (e.g. shrub removal, logging/timber extraction and over grazing in the late Holocene) were the dominant driver for the extensive removal of soils from hillslopes in many regions (*Fuchs et al.*, 2004; *Fuchs*, 2007; *van Andel et al.*, 1990). These conclusions differ from studies in the Negev Desert in Israel which found that most of the hillslope loess apron was eroded in the early Holocene, prior to significant human settlement (*Avni et al.* 2006). This finding suggests that the degradation of soil from the Negev Desert hillslopes, where such existed, was driven by climatic, rather than anthropogenic processes. Consequently, there is an ongoing debate in the literature regarding the drivers of the extensive soil depletion in Mediterranean and southern European hillslopes.

From a soilscape evolution point of view, aeolian dominated soilscales differ from bedrock-weathering dominated soilscales in several ways. In bedrock-weathering systems *in situ* weathering rates decrease exponentially with soil depth (*Gilbert*, 1877; *Ahnert*, 1977), thus regulating soil production as a function of regolith thickness (*Heimsath et al.*, 1997). Weathering of regolith and soil leads to vertical particle size distribution with finer particles closer to the surface as a

function of the soil and regolith age, namely time exposed to weathering (Yoo and Mudd 2008). At the surface, armouring can develop by size-selective entrainment (Kim and Ivanov, 2014) or vegetation shielding, which limits sediment transport by overland flow (Willgoose and Sharmeen, 2006). Given sufficient time and in the absence of vertical mixing due to pedoturbation, these processes - depth dependent weathering, vertical self-organization and surface armouring - will stabilize the soilscape leading to steady-state or dynamic equilibrium conditions (Cohen *et al.*, 2013 & 2015). In aeolian dominated landscapes these controls on soil production and transport are largely ineffective as: (1) much of the soil is transported to the system as airborne sediments, i.e., no depth dependency; and (2) fine and highly erodible material is continuously deposited on top of older surface soils which limits the potential for surface armouring and vertical self-organization.

The differences between aeolian and bedrock-weathering dominated soilscales lead us to conclude that traditional (i.e. bedrock weathering originated) soilscape evolution analysis is inappropriate for investigating the history of the aforementioned loess soilscales. In Cohen *et al.* (2015) we developed a soilscape evolution model (mARM5D) to study the differences and interactions between aeolian and bedrock weathering soil production on a synthetic 1D hillslope. In that paper we have found that bedrock weathering dominated soilscales are considerably more stable and showed much lower spatial (aerial) variability in soil depth and particle size distribution (PSD). We proposed that aeolian-dominated landscapes are more responsive to environmental changes (e.g., climatic and anthropogenic) compared with bedrock-weathering landscapes.

Here we use mARM5D to investigate an aeolian dominated field-site in central Israel located at the margin between Mediterranean and arid climates and with long history of human settlement. We introduce anthropogenic and climatic drivers to investigate the potential importance of temporal dynamics on soilscape evolution. We focus our analysis in this paper on the differences between Fluvial (rilling, hillslope wash and concentrated flow) and Diffusive (soil creep) hillslope sediment transport mechanisms. We seek to gain better understanding about how these sediment transport mechanisms affect soilscape evolution in this soilscape. This is important as: (1) each transport mechanism is affected differently by climatic/anthropogenic drivers; and (2) we do not know what is the potential contribution/importance of each mechanism on soilscape evolution.

2. Methodology

2.1 Field site and measured data

The field-site (Long Term Ecological Research, LTER, near Lehavim in the Northern Negev, Israel; 31°20' N, 34°45' E; Figure 1) is situated on the desert margin between a Mediterranean climatic regime to the north and an arid climatic regime to the south (note changes in green vegetation in Figure 1a). The area of the site is 0.115 km². This region has shifted between these two climatic regimes throughout the Pleistocene and Holocene (Vaks *et al.*, 2006). This region has also seen varying degrees of human settlement and agricultural activity throughout the late Holocene. The history of this region (both

human and natural) gives us a unique opportunity to study how climatic and anthropogenic drivers may have affected hillslope geomorphology resulting in the soil-depleted landscape we see today.

The LTER site is located in Aleket basin with an average rainfall of 290 mm per annum. The mean annual temperature is 20.5°C, with a maximum of 27.5°C and a minimum of 12.5°C. The terrain is hilly and the area is divided by an east-west flowing ephemeral stream. The dominant rock formations are Eocenean limestone and chalk with patches of calcrete. Soils are brown lithosols and arid brown loess. Much of the loess was eroded from the hillslopes and deposited in the valleys (several meters deep in some locations). The vegetation is characterized by scattered dwarf shrubs (dominant species *Sarcopoterium spinosum*) and patches of herbaceous vegetation, mostly annuals, are spread between rocks and dwarf shrubs (Svoray *et al.* 2008). The herbaceous vegetation is highly diverse, mostly composed of annual species (Svoray and Karnieli 2011). At the research site a typical convex shaped slope was chosen for testing model predictions (Figure 1d).

A dataset of measured topography and soil parameters at the study site (including soil depth distribution and a Digital Elevation Model; DEM) is available from a previous study (Sela *et al.* 2012). A soil depth map (Figure 2) was compiled using Ordinary Kriging interpolation of 550-point measurements. An orthophoto (at 10 cm² pixel resolution) was used to classify exposed rock and assign zero depth to the interpolation map. The DEM used in this study was obtained from 700 measured points (at approximately 10 meter intervals) using a laser theodolite (SOKIA Inc. Total Station) and interpolated using Ordinary Kriging to a horizontal resolution to 2 x 2 meter pixel resolution for the mARM5D simulations. From this DEM a D8 flow direction, Dinf (D-infinity algorithm; Tarboton, 1997) slope (m/m) and Dinf contributing area layers were calculated using the TauDEM tool (Tarboton, 2010).

2.2 Application of mARM5D to Lehavim site

In Cohen *et al.* (2015) we developed a dynamic soil evolution model (mARM5D) to simulate soil physics as a state-space system as an extension of the mARM3D model (Cohen *et al.*, 2009; 2010). mARM5D is a modular and computationally efficient modelling platform that explicitly simulates three spatial dimensions in addition to a temporal dimension and a PSD (hence the 5D suffix). The cellular model simulates soil evolution over a given landscape by describing changes in PSD in a finite number of equally thick soil profile layers (size and number are defined by the user) in each grid-cell.

The mARM framework introduced a novel implementation of physically-based equations using transition matrices that express the relative change in spatially and temporally explicit PSD vectors. This concept greatly improves the model computational efficiency and modularity but is challenging to describe in full. Below we describe the mARM5D physically-based equations that include the parameters that are modified in the simulation scenarios we analysed in this paper. A full description of the mARM model architecture as a platform to mARM5D can be found in the following publications: The model weathering component was explored in Cohen *et al.* (2010), its spatiotemporal algorithms in Cohen *et al.* (2013) and

its aeolian and sediment transport components in Cohen et al. (2015). In Cohen et al. (2015) also outline and discuss the model assumptions.

Here, we simulate the spatial and temporal changes in PSD as resulting from: (1) physical weathering of bedrock and soil particles in each profile-layer; (2) aeolian deposition on top of the surface layer; (3) size-selective entrainment and deposition by overland flow (generally referred to here as fluvial sediment transport) from/on the surface layer; and (4) non size-selective diffusive sediment transport (creep) both on the surface and within the soil profile.

2.1.1 Fluvial transport

For each grid-cell, the top layer is the surface layer exposed directly to size-selective erosion. Sediment transport capacity over a timestep (q_s , m³/m) at the surface is calculated using a modification of the TOPOG model (TOPOG, 1997; Merritt et al., 2003) sediment transport equation

$$q_s = e \frac{q^{n_1} S^{n_2}}{(s-1)^2 d_{50}^{n_3}} \Delta t \quad (1)$$

where e is an empirical erodibility factor, q is discharge per unit width (m³/s/m), S is slope (m/m), d_{50} is the median diameter (m) of the material in the surface layer, s is the specific gravity of sediment ($s=2.65$; kg/m³), n_1 , n_2 and n_3 are calibration parameters and Δt is the iteration timestep size (e.g. 0.1 year). The units of erodibility parameter e are a function of the calibration exponents n_1 , n_2 and n_3 and are defined such that the units of q_s are the ones specified. We used here $n_1=1$ and $n_2=1.2$ based on a calibration in Cohen et al. (2009) and modified n_3 to 0.5 (from 0.025) to adjust for the very fine-grained aeolian sediment.

Discharge (q ; m³/s/m) is

$$q = \left[\frac{A}{A_p} \right]^{n_4} \frac{Q}{(A_p)^{0.5}} \quad (2)$$

where Q (m³/s) is the excess hillslope runoff variable, A is the upslope contributing area (m²), A_p is the area of a grid cell unit (m²) and n_4 is a constant relating runoff as a function of contributing area. In Cohen et al. (2010 and 2015) the relationship between contributing area and runoff discharge was assumed to be linear ($n_4=1$). This assumption could not be justified in our field-site as Yair and Kossovsky (2002) showed that runoff generation in this region does not increase linearly downslope. Using an extensive parametric study (not presented here) we have found that $n_4=0.1$ leads to best approximation of observed soil distribution. We will discuss this later. Water is routed to a neighbouring grid-cell with the 'steepest descent' (D8) algorithm (O'Callaghan and Mark, 1984).

Sagy Cohen 11/21/2016 11:20 AM

Deleted: $q_s = e \frac{q^{n_1} S^{n_2}}{(1-s)^2 d_{50}^{n_3}} \Delta t$

Sagy Cohen 11/21/2016 11:20 AM

Deleted: .

Sagy Cohen 11/21/2016 11:20 AM

Deleted: We therefore use

Sagy Cohen 11/21/2016 11:20 AM

Deleted: in

Sagy Cohen 11/21/2016 11:20 AM

Deleted: study

Sagy Cohen 11/21/2016 11:20 AM

Deleted: neighboring

Sagy Cohen 11/21/2016 11:20 AM

Deleted:)

2.1.2 Diffusion transport

Traditionally, equations of two-dimensional diffusive transport calculate sediment discharge as a linear relationship to slope, soil thickness and a diffusion coefficient (e.g. the creep model of *Culling*, 1963, or the viscous flow model of *Ahnert*, 1976) and, if the soil is explicitly modelled at all, diffusion is considered independent of depth through the profile. Simulation of the soil profile in mARM5D is novel as it explicitly calculates diffusive transport for each soil profile layer. Based on *Roering* (2004), the diffusivity is assumed to decrease exponentially with depth below the soil surface:

$$D_{c_l} = \exp(-\lambda h_l) \quad (3)$$

where D_{c_l} is the fraction of diffusion rate for the layer l relative to the diffusion rate at the surface D_s (l), h_l is the mean depth (m) of profile layer l relative to the surface and λ is a calibration parameter. We used $\lambda=0.02$ based on *Fleming and Johnson* (1975) and *Roering* (2004). The surface diffusion sediment transport rate (D_s ; m) is:

$$D_s = \left(\frac{S}{S_a}\right)^\beta D_o \Delta t \quad (4)$$

where D_o is the surface diffusivity (m/y) and S_a is the adjustment slope, the average slope in which D_o was measured/estimated. Here we use $S_a=0.2$ which approximate our field site average slope. Using an extensive sensitivity analysis we have found that $\beta=0.1$ yielded the best approximation to our field site's soil distribution. This value differs from the typical assumption of a linear relationship between slope and diffusion ($\beta=1$), suggesting that the influence of topographic slope in this soilscape is much lower. We will discuss this later. The removal of material due to diffusion from a given layer is calculated as the proportion of the layer's movable material (expressed in the model as a PSD vector g_l) that has been displaced at each iteration:

$$\underline{g}_{l+1} = \underline{g}_l - \left[\underline{g}_l \left(\frac{D_s}{\sqrt{A_p}} \right) D_{c_l} \right] \quad (5)$$

2.1.3 Aeolian deposition

Sediment, with a user-defined grading distribution (\underline{g}_a), is added to the surface layer. The aeolian deposition rate (K_a ; mm/yr) is assumed to be spatially uniform:

$$h_s \underline{g}_{s_{t+1}} = h_s \underline{g}_s + K_a \underline{g}_a \quad (6)$$

where \underline{g}_s is the vector for the surface layer PSD and h_s is the thickness of the surface layer. We use the same PSD as in the fine-grained simulation in *Cohen et al.*, (2015), with a $d_{50}=0.06$ mm (derived from *Bruins and Yaalon*, 1992)

Sagy Cohen 11/21/2016 11:20 AM

Deleted: $D_l = D_s [\exp(-\lambda h_l)]$

Sagy Cohen 11/21/2016 11:20 AM

Deleted: D_l (m/y)

Sagy Cohen 11/21/2016 11:20 AM

Deleted: diffusive transport

Sagy Cohen 11/21/2016 11:20 AM

Deleted: D_s is

Sagy Cohen 11/21/2016 11:20 AM

Deleted: (maximum) diffusive sediment transport rate (m/y)

Sagy Cohen 11/21/2016 11:20 AM

Deleted: /y

Sagy Cohen 11/21/2016 11:20 AM

Deleted: Sediment flux for each

Sagy Cohen 11/21/2016 11:20 AM

Deleted: can be

Sagy Cohen 11/21/2016 11:20 AM

Deleted: by multiplying D_s by

Sagy Cohen 11/21/2016 11:20 AM

Deleted: volume and

Sagy Cohen 11/21/2016 11:20 AM

Deleted: bulk density of

Sagy Cohen 11/21/2016 11:20 AM

Deleted: soil. We assumed constant volume and bulk density.

. For the sake of simplicity, aeolian sediment is assumed to originate from outside the system and no aeolian erosion is considered within the simulated domain. This means that K_a is, in our case, the aeolian sediment accumulation (deposition) rate.

5 2.3 Simulation scenarios

Four model parameters are driven by climate and anthropogenic changes:

1. e - Surface Erodibility (equation 1);
2. Q - Runoff (equation 2);
3. D_θ - Surface diffusive transport rate (equation 4);
4. K_a - Aeolian deposition rate (equation 6).

The effect of climate and anthropogenic change on the model parameters represent our best estimates based on the literature for this semiarid region. They can be summarized as:

1. Wetter climatic conditions allow for higher vegetation cover and thus lower surface erodibility and runoff generation (e and Q respectively) (Goodfriend, 1987, Zilberman, 1992 and Avni et al., 2006).
 2. During wetter climatic condition colluvial processes are more intensive (Goodfriend, 1987 and Zilberman, 1992), translating into a higher diffusive sediment transport rate (D_θ).
 3. During wetter climatic condition aeolian deposition rates are higher (K_a) (Horowitz, 1979 and Bowman et al., 1986).
 4. Human activities in this area reduce vegetation cover on the hillslopes (mostly by grazing), enhancing the effect of the dry climate during the Holocene (Fuchs et al., 2004), increasing e and Q and decreasing D_θ and K_a .
- Using these assumptions we divided the simulation scenario into three homogenous periods (Figure 3 and Table 1) based on Vaks et al. (2006):
- P1- Late Pleistocene (80-12 kyr BP): wetter climatic period – a factor of 0.1 for erosivity and runoff (e and Q respectively), scale of 2 for diffusion (D_θ) relative to modern rates and a maximum rate for aeolian deposition (K_a).
- P2 - Early Holocene (12-8 kyr BP): dry climatic period - scale of 0.2 for e and Q , factor of 2 for D_θ (unchanged from P1) relative to modern rates and scale of 0.5 for K_a relative to its P1 (maximum) rate.
- P3 - Late Holocene (8-0 kyr BP): increasingly drier climate with human activity - scale of 1 (maximum) for e and Q , scale of 1 for D_θ and factor of 0.1 for K_a relative to its P1 (maximum) rate.

2.4 Simulated processes and calibration

- Three site-scale simulations are analyzed in this paper:

Sagy Cohen 11/21/2016 11:20 AM

Deleted: 3 and

Sagy Cohen 11/21/2016 11:20 AM

Deleted: 5

S1- sediment transport is simulated only by fluvial processes;

S2- sediment transport is simulated only by diffusion;

S3- sediment transport is simulated by both diffusive and fluvial mechanisms.

Soil is produced and supplied by both bedrock weathering and aeolian deposition. Soil production by bedrock weathering

5 was assumed to be small relative to loess accumulation rate due to the dominance of limestone geology in the site. Limestone bedrock typically results in limited soil production by weathering except for producing a Mollisol, which is not simulated, and rock fragments, which are simulated. Weathering rate (P_0 in equation 5) is thus set to spatially and temporally constant value of 0.01 mm/y. Maximum aeolian deposition rate (during P1 simulation scenario period) is spatially constant and set to 0.1 mm/y based on *Bruins and Yaalon* (1992).

10 Initial values during the P3 period (most modern) for Q was estimated based on *Eldridge et al.* (2002) and *Yair and Kossovski* (2002) and for D_0 based on *Carson and Kirkby* (1972). Adjusting these two parameters controls the ratio between the fluvial and diffusive sediment transport mechanisms. The values of these parameters were refined by an extensive parametric study to best match observed soil depth distribution. The best match was for $Q=0.0066 \text{ m}^3/\text{y}$ and $D_0=6 \text{ mm/y}$ for the P3 period (Table 1).

15 For the S1 and S2 simulations, the Q and D_0 parameters were adjusted to yield a similar average soil depth as the S3 simulation. This adjustment ensures that the differences observed between the three simulations are mainly due to differences in sediment transport mechanism, not the accumulative variations in sediment transport rate. For S1 Q was adjusted to $0.017 \text{ m}^3/\text{y}$ and D_0 was set to 0 (no diffusive transport; Table 1). For the S2 simulation D_0 was adjusted to 10.75 mm/y and Q was set to 0 (no fluvial transport).

20

3. Results

3.1 Field Site Application

For the fluvial simulation (S1), the P1 period, with low runoff and surface erodibility and high aeolian deposition (Figure 3), produced deep soils on the hillslopes (up to 200 cm; Figure 4a-b). During P2, with higher runoff and surface erodibility rates

25 and lower aeolian deposition rate (by a factor of 2), soil is slowly eroding primarily from the lower sections of the hillslopes (Figure 4c-d). Erosion greatly intensifies during P3 due to further increase in runoff and surface erodibility rates and lowering in aeolian deposition rate (by a factor of 5). By the end of P3, most of the thick hillslopes loess apron has been eroded (Figure 4f) leaving two clusters of relatively deep soils (about 150 cm deep) on the interfluvial, as well as quite extensive shallow aprons (about 50 cm deep) at the top and middle sections of the hillslopes. The rest of the hillslope is covered with a shallow soil layer (<20 cm) with no exposed bedrock. This soil distribution does not correspond well with observed soil depth (Figure 2) which exhibits a high degree of exposed bedrock at the top section of the hillslopes and the interfluvial and deeper soils at the lower parts of the hillslopes.

30

The diffusive simulation (S2) yielded long straight bands of soil deposition along parts of the [simulation domain](#), [\(Figure 5\)](#). These bands follow the D8 flow direction input and are only apparent in the diffusive simulation. [This is because soil transport away from a grid cell is not affected by its upstream contributing area \(only its local slope\) for the diffusive mechanism while deposition will be higher in cells with greater flow accumulation \(more sediment has the potential of being transported to it\). As a result cells along concentrated flow paths may result in deep soil deposited from upstream cells. S2 is an extreme diffusion scenario, combining highly mobile sediment influx \(aeolian deposition\) with high diffusion rates \(enhanced by the high topographic slopes in this field site\). While more moderate landscapes and rates will minimize these artefacts improvement to the diffusion transport mechanism is likely needed and be the focus of future research.](#)

The P1 period for the S2 simulation, with high diffusive and aeolian deposition rates, produced soil accumulation at lower sections of the hillslopes (Figure 5a-b). These deposition features are over 100 cm deep at the footslope and are decreasing in depth upslope. The upper sections of the hillslopes are covered with a shallow loess apron (< 20 cm) with narrow bands of exposed bedrock (white color) along the interfluvium. During P2, aeolian deposition rate decreased while the diffusive rate remained high (Figure 3). This leads to erosion of the upslope deposition bands resulting in a slight decrease in their spatial extent (Figure 5c-d). The extent of the exposed bedrock feature along the crest and down the hillslopes increased. During P3, the diffusive rate decreases by a factor of 2 and aeolian deposition by a further factor of 5. The main impact of this reduced soil supply is an extensive degradation of the thin loess apron on the hillslopes (Figures 5e-f). The deposition bands at the bottom of the hillslopes are relatively unaffected. Final soil distribution (Figure 5f) better corresponds with the measured soil distribution (Figure 2) compared with the S1 simulation (Figure 4f). Measured soil depth tends to be more heterogeneous and widespread and does not show extremely localized deposition features at the footslopes.

In the combined fluvial and diffusive simulation (S3) the P1 period shows deep soil features, about 150 cm, covering most of the intermediate and lower sections of the hillslopes (Figure 6a-b). With an exception of a thin band of deep soils near the crest, the upslope parts are covered with a shallow loess apron (less than 15 cm). The changes during P2 (aeolian deposition decrease by a factor of 2, fluvial rate increase by a factor of 2 and diffusive rate remain high) initially led to degradation of the loess apron at the upper parts of the hillslopes (Figure 6c). Once the loess apron has been completely removed, the deposition features at the lower section of the hillslopes start to erode (Figure 6d). This trend accelerates during P3 due to the sharp decrease in aeolian deposition rate. The increase in fluvial rate by a factor of 5 while diffusive rate decreases by a factor of 2 (Figure 3) leads to greater erosion at the bottom parts of the deposition features (Figure 7e-f). The resulting soil distribution better corresponds with measured soil distribution: exposed bedrock at the top and bottom parts of the hillslopes with a mostly shallow band of soil at the middle part of the hillslopes. The considerable changes in soil depths during P3 shows that intense but relatively short changes in external drivers (representing anthropogenic alterations in this study) can be significant for this soilscape evolution.

Sagy Cohen 11/21/2016 11:20 AM

Deleted: .

Sagy Cohen 11/21/2016 11:20 AM

Deleted: This seems to be because diffusive rate is highest during the P1 period in which aeolian deposition is also highest leading to the formation of deep deposition features down the flow lines. This observation is in contrast with the fluvial simulation in which highest fluvial transport rates occur following a long period of extensive loess accumulation on the hillslopes (Figure 4b). This result emphasizes the importance of temporal dynamics in soil production and erosion.

3.2 Transect (1D) Analysis

Soil depth evolution was plotted along a transect on the northwestern facing hillslope (thick black line with crossing short lines in Figures 1c and 4-6), focusing on the last 16 kyr of the simulations (the most dynamic period of these simulations).

The S1 profile (Figure 7a) gradually thins toward the footslope while the S2 (Figure 7b) profile is very thin at the top of the hillslope and then thickens considerably from nearly zero depth to about 190 cm over a stretch of less than 5 m. The S3 simulation (Figure 7c) has also resulted in a steep step in soil depth between the upper and lower parts of the hillslope. However, the S3 simulation resulted in considerable variability in soil depth at the footslope. In the S1 simulation the hillslope profile changes considerably during the plotted 16 kyr while the S2 profile displays only minor variation and S3 varies mainly at the bottom of the hillslope. The S1 hillslope profile initially erodes evenly in space but during P3 it shows increased erosion rate at the top of the hillslope. This trend is also visible in S3.

The final (0 kyr BP) hillslope profile for S3 has a nearly 35 m long exposed bedrock section at the top part of the hillslope (also visible in Figure 6f) followed by a deposition section with a downslope decreasing soil depth (from about 100 to 10 cm at the bottom of the hillslope). This profile has a number of both steep and shallow steps in soil depth (from more than a 100 cm to less than 10 cm) which are commonly observed in the Lehavim field-site. The measured soil depth profile along the transect (Figure 7d) is shallower and displays a smoother (it is an interpolation of measurement points) transition between the erosive and deposition parts of the hillslope. Overall the S3 soil-depth profile (Figure 8c) shows similar trends to the measured soil depth (Figure 7d). Particularly notable is the correspondence in the location of the mid-slope soil depth depression.

4. Discussion

Roering (2008) simulated soilscape evolution in a soil-mantled and vegetated landscape in northwestern U.S. He studied a number of diffusive sediment transport mechanisms and found that the best fit for the observed landform and soil distribution (increase in soil depth with slope angle downslope) was a nonlinear and soil depth-dependent model. He argued that soil thickness controls the magnitude of biogenetic activity (e.g. bioturbation) which drives sediment transport. In semiarid soil-depleted environments, landscape evolution and soil distribution was also found to be related to soil depth but by a different mechanism. *Saco et al.* (2007) simulated a semiarid and soil-depleted landscape and showed that soilscape evolution under water-limited conditions tend to follow a source-sink dynamics in which soil bands (which are deep enough to support vegetation) will act as a sink for water and sediment fluvially transported (surface wash) from bare intermediate sections between the vegetated bands.

The Lehavim LTER field site, under modern climatic conditions, is under a water-limited regime resulting in vegetation patches acting as sinks to the exposed bedrock section on the hillslope (*Svoray et al.*, 2008; *Svoray and Karnieli*, 2011) leading to micro-topographic variability. The site's soilscape is also characterized by a general trend of increasing soil depths

downslope. This suggests an intriguing interplay between semiarid and soil-mantled soilscape evolution. Our results show that during wetter periods (with greater aeolian deposition rates, P1) soil was thickening at the downslope direction (Figure 5b and Figure 6c). During the following drier periods (P2 and P3) the bottom part of the hillslopes started eroding resulting in a soil distribution where the middle part of the hillslope shows the deepest soil (the mid-slope depression; Figure 5 and 6).

5 Simulated fluvial sediment transport led to a somewhat unusual soil distribution in which soil is thickest at the interfluvial (Figure 4). Hints of this kind of soil distribution are evident in the Lehavim LTER site (e.g. north sections of both northwest and southeast facing hillslopes; Figure 2) but are not as prominent as the S1 simulation predicted. Diffusive transport tended to produce localized deep deposition features at the bottom of the hillslopes. Evidence of this type of soil distribution can also be seen in this field-site (primarily on the southeast facing hillslope; Figure 2) though not as deep and localized as the
10 S2 simulation (diffusive only sediment transport; Figure 5) produced. Only by simulating both fluvial and diffusive transport mechanisms can the model correctly simulate the observed soil distribution. Even though simulating both fluvial and diffusive sediment transport is common practice in many landscape-evolution models (*Tucker and Hancock, 2010*), the interaction between them is often uncertain (*Hancock et al., 2002*), particularly under unique circumstances like in this field-site: fine-grained aeolian-dominated soils with high degree of temporal variation in soil supply.

15 [Cohen et al., \(2015\)](#) used the mARM5D model to investigate the differences between bedrock and aeolian dominated soilscape evolution. While the results of that study cannot be directly compared to the results presented in this paper (due to differences in simulation domains and parameterization), they help support some of the assertions proposed by this study. The results in this paper show that different parts of the hillslopes tend to be dominated by one of the two transport mechanisms; diffusion at the top and fluvial at the bottom. [Cohen et al., \(2015\)](#) found an opposite trend for bedrock
20 weathering dominated soils. In bedrock weathering dominated soils heterogeneity in PSD along the soil profile and selective entrainment by overland flow will result in less erosive (armoured) surface in response to increasing fluvial rates. Therefore increases in runoff rates downslope will not yield a considerable increase in sediment transport (rather an increasingly coarse, source-limited, surface). In aeolian dominated soils the absence of such a mechanism means that increasing runoff downslope will, in the absence of other factors, result in increasing fluvial transport rates downslopes
25 hence the dominance of this transport mechanism at the bottom part of aeolian dominated hillslopes.

In Cohen et al. (2015) we have also found that heterogeneity in soil distribution, derived from dominance of one of the two sediment transport mechanism, were considerably more pronounced in aeolian-dominated soils. Generally, fluvial sediment transport in bedrock weathering dominated soils, given enough time and pedoturbation stability, will lead to a source-limited flow regime which is in equilibrium with soil production rates (and thus soil depth; Cohen et al., 2015). This
30 helps explain the patchy soil distribution in aeolian-dominated soils and support our assertion in Cohen et al. (2015) that aeolian dominated soils are more responsive (susceptible) to environmental changes.

Diffusion rate for this field site was found (based on an extensive parametric study) to have a weak and nonlinear relationship with topographic slope ($\beta=0.1$ in Eq. 4). [Similarly, the relationship between contributing area and discharge \(Eq. 2\) was found to be a weak and nonlinear relationship \(\$n_4=0.1\$ \). These differ from the usual assumption of linearity and may](#)

Sagy Cohen 11/21/2016 11:20 AM

Deleted: The results

Sagy Cohen 11/21/2016 11:20 AM

Deleted: In

Sagy Cohen 11/21/2016 11:20 AM

Deleted: we

Sagy Cohen 11/21/2016 11:20 AM

Deleted: This differs

Sagy Cohen 11/21/2016 11:20 AM

Deleted: (e.g. [ref.](#))

be due to the aeolian characteristics of the site's soilscape (fine PSD, absence of armouring mechanism, etc.) or, more likely, may be attributed to the relatively steep and concave-down (increase in gradient downslope) characteristics of this field site.

Concave-down hillslope means that slope gradients are highest at the lower parts of the hillslope. A linear relationship between slope and diffusion rate, in conjunction with increasing fluvial rates with contributing area, will therefore not allow for soil to accumulate at the lower part of the hillslope, as observed in our field site. Catena shaped hillslopes can be assumed to have a linear relationship, as slopes are lower at the footslope and toeslope. This will be the focus of a future study.

The overarching goal of this study is the investigation of the history of this region's soilscape evolution in the context of anthropogenically and climatologically driven soil depletion from hillslopes in Europe and southern Israel. The results demonstrate that soil distribution in our field site are highly susceptible to short environmental change. This is in contrast to the results of Cohen et al. (2013) which demonstrated that the response of bedrock weathering dominated soilscares to climatic shifts will be a slow transition toward a new steady-state conditions. From this we can again conclude that aeolian dominated soilscares are more susceptible to environmental change and thus even a relatively small change will lead to considerable alterations. The sharp increase in soil erodibility in the P3 stage representing anthropogenic activity have lead to the good agreement between our simulation results and the observed soil depth distribution at the field. This suggests that a) soil cover in our field site's hillslopes might have been more extensive during the early Holocene, and b) anthropogenic activity could have led to the soil-depleted hillslopes we observe today.

Soilscape evolution and distribution is typically calculated as a function of landscape topography (as was done here). However, we may also think of an opposite interaction, the effect of soil distribution on landscape evolution (i.e. topography) as studied by Roering (2008) on a soil-mantled landscape. The concave shape of the hillslope in this site may be linked to soil thickening downslope. Thicker soil in this soil-depleted landscape is likely to increase rock weathering (following the 'hump' weathering rate concept), which in this site (limestone dominated lithology) is mostly dissolution, leading to topographic lowering. This process is evident in the micro-topography along the hillslopes (likely propagated by soil/vegetation patches) and from Saco et al. (2007) which showed that soil/vegetation bands alter landscape morphology in water-limited environments. This suggests that the massive influx of aeolian sediment during the late-Pleistocene and early-Holocene may have considerably altered the morphology of this landscape, suggesting a strong coupling between soil production and landscape evolution, a hypothesis that needs to be further investigated.

5. Conclusions

Fluvial and diffusive sediment transport mechanisms lead to distinctively different soilscape evolutionary paths. Under erosive conditions - when transport rates are higher than sediment supply rates - the fluvial mechanism resulted in downslope thinning in soil depth while the diffusion led to downslope thickening. Neither mechanism was able to produce a soil distribution corresponding to that observed in our field-site. Only when both fluvial and diffusive sediment transport

mechanisms were modeled, a reasonable correspondence was achieved. While soilscape are generally thought off as resulting from both transport mechanisms, this and previous studies demonstrates that fluvial-diffusion coupling is more pronounced in aeolian dominated soilscape.

The results also point to soil distribution features that are indicative of the different sediment transport mechanism. It suggests that, for our semiarid aeolian-dominated field-site, diffusive transport is the dominant mechanism at the top part of the hillslope and fluvial processes are dominant at the. This is in contrast to bedrock weathering dominated soilscape in which the opposite was observed as increased surface armouring downslope reduces fluvial transport.

Temporal variability in external drivers was shown to be a significant factor in this site's soilscape evolution. This demonstrates the importance of explicitly accounting for geomorphic processes and temporal variability in environmental and anthropogenic dynamics in order to understand the soilscape history, particularly in highly pedogenetic, anthropogenic and climatologically dynamic regions.

This study advanced our understanding of this region's soilscape evolution by elucidating the sediment transport mechanism that may have led to the soil distribution we observe today. The results suggest that relatively swift environmental changes in the late Holocene (i.e. anthropogenic activity) could have considerably changed the site's soil distribution from a soil-mantled hillslopes (albeit with thin loess apron in many locations) to the soil-depleted hillslopes we observe today. Additional research is needed (and is ongoing) to better confine the rates and spatiotemporal dynamics of soil erosion and development in this site.

Acknowledgments

This research was supported by the Israel Science Foundation (ISF) (grant 1184/11). GRW was supported by an Australian Research Council Australian Professorial Fellowship.

References

- Ahnert, F., (1977), Some comments on the quantitative formulation of geomorphological process in a theoretical model, *Earth Surface Processes*, 2, 191–201.
- Almogi-Labin, A., M. Bar-Matthews, D. Shriki, E. Kolosovsky, M. Paterne, B. Schilman, A. Ayalon, Z. Aizenshtat, and A. Matthews (2009), Climatic variability during the last similar to 90 ka of the southern and northern Levantine Basin as evident from marine records and speleothems, *Quaternary Science Reviews*, 28(25-26), 2882-2896.
- Avni, Y., N. Porat, J. Plakht, and G. Avni (2006), Geomorphic changes leading to natural desertification versus anthropogenic land conservation in an arid environment, the Negev Highlands, Israel, *Geomorphology*, 82(3-4), 177-200.

- Bowman, D., A. Karnieli, A. Issar, and H. J. Bruins (1986), Residual Colluvio-aeolian Aprons in the Negev Highlands (Israel) as a Paleo-Climatic Indicator, *Palaeogeography Palaeoclimatology Palaeoecology*, 56(1-2), 89-101.
- Bruins, H.J., and D.H. Yaalon (1992), Parallel advance of slopes in aeolian loess deposits of the northern Negev, Israel, *Israel Journal of Earth Sciences*, 41, 189-199.
- 5 Butzer, K. W. (2005), Environmental history in the Mediterranean world: cross-disciplinary investigation of cause-and-effect for degradation and soil erosion, *Journal of Archaeological Science*, 32(12), 1773-1800.
- Carson, M. A., and M. J. Kirkby (1972), *Hillslope Form and Process*, 475 pp., Cambridge Univ. Press, Cambridge, U.K.
- Cohen, S., G. Willgoose, and G. Hancock (2013), Soil-landscape response to mid and late Quaternary climate fluctuations based on numerical simulations, *Quaternary Research*, 79 (3): 452-457. doi: 10.1016/j.yqres.2013.01.001
- 10 Cohen, S., G. Willgoose, and G. Hancock (2010), The mARM3D spatially distributed soil evolution model: three-dimensional model framework, and analysis of hillslope and landform responses, *Journal of Geophysical Research-Earth Surface*, 115, F04013, doi:10.1029/2009JF001536.
- Cohen, S., G. Willgoose, and G. Hancock (2009), The mARM spatially distributed soil evolution model: A computationally efficient modeling framework and analysis of hillslope soil surface organization, *Journal of Geophysical Research-Earth Surface*, 114, F03001, doi:10.1029/2008JF001214.
- 15 Cohen, S., G. Willgoose, T. Svoray, G. Hancock, and S. Sela (2015), The effects of sediment transport, weathering and aeolian mechanisms on soil evolution, *Journal of Geophysical Research-Earth Surface*, 120: 260-274. DOI: 10.1002/2014JF003186
- Eldridge, D. J., E. Zaady, and M. Shachak (2002), Microphytic crusts, shrub patches and water harvesting in the Negev Desert: the Shikim system, *Landscape Ecology*, 17(6), 587-597.
- 20 Fleming R. W. and A. M. Johnson (1975), Rates of seasonal creep of silty clay soil, *Quarterly Journal of Engineering Geology*, 8: 1-29.
- Fuchs, M. (2007), An assessment of human versus climatic impacts on Holocene soil erosion in NE Peloponnese, Greece, *Quaternary Research*, 67(3), 349-356.
- 25 Fuchs, M., A. Lang, and G. A. Wagner (2004), The history of Holocene soil erosion in the Phlous Basin, NE Peloponnese, Greece, based on optical dating, *Holocene*, 14(3), 334-345.
- Gilbert, G.K., (1877), *Report of the Henry Mountains (Utah)*, US Geographical and Geological Survey of Rocky Mountains Region, US Government Printing Office, Washington DC. 169pp.
- Goodfriend, G. A. (1987), Chronostratigraphic studies of sediments in the Negev desert, using amino acid epimerization analysis of land snail shells, *Quaternary Research*, 28(3), 374-392.
- 30 Hancock G R, G R Willgoose K G Evans, 2002. Testing of the SIBERIA landscape evolution model using the Tin Camp Creek, Northern Territory, Australia, field catchment, *Earth Surface Processes and Landforms*, 27, 125-143.
- Heimsath, A.M., Chappell, J.C., Spooner, N.A., Questiaux, D.G., (2002), Creeping soil. *Geology*. 30(2): 111-114.

- Heimsath, A. M., Dietrich, W. E., Nishiizumi, K., and Finkel R. C., (1997), The soil production function and landscape equilibrium, *Nature*, 388(6640), 358-361.
- Horowitz, A., (1979), The Quaternary of Israel: New York, Academic Press, 394 p.
- Hughes, M. W., Almond, P.C., Roering, J. J., and Tonkin, P. J., (2010), Late Quaternary loess landscape evolution on an active tectonic margin, Charwell Basin, South Island, New Zealand, *Geomorphology*, 122, 294-308.
- Hughes, M. W., Schmidt, J., and Almond, P.C., (2009), Automatic landform stratification and environmental correlation for modeling loess landscape in North Otago, South Island, New Zealand, *Geoderma*, 149, 92-100.
- Istanbulluoglu, E., D. Tarboton, R. Pack, and C. Luce (2004), Modeling of the interactions between forest vegetation, disturbances, and sediment yields, *J. Geophys. Res. -Earth Surf.*, 109(F1), F01009, doi: 10.1029/2003JF000041.
- Kim, J., and V. Y. Ivanov (2014), On the nonuniqueness of sediment yield at the catchment scale: The effects of soil antecedent conditions and surface shield, *Water Resour. Res.*, 50(2), 1025–1045, doi:10.1002/2013WR014580.
- Langbein, W.B. and Schumm, S.A., (1958), Yield of sediment in relation to mean annual precipitation, *Transactions of the American Geophysical Union*, 39, 1076-1084.
- Ludwig, J., B. Wilcox, D. Breshears, D. Tongway, and A. Imeson (2005), Vegetation patches and runoff-erosion as interacting ecohydrological processes in semiarid landscapes, *Ecology*, 86(2), 288-297, doi: 10.1890/03-0569.
- McFadden, L.D. and P.L.K. Knuepfer (1990), Soil geomorphology: the linkage of pedology and superficial processes ,in: P.L.K. Knuepfer, L.D. MacFadden (Eds.), Soils and Landscape Evolution, *Geomorphology*, 3, 197–205.
- Merritt W, Letcher R, Jakeman A. 2003. A review of erosion and sediment transport models. *Environmental Modelling & Software* 18: 761-799.
- Minasny, B., and McBratney, A.B. (2006), Mechanistic soil-landscape modelling as an approach to developing pedogenesis classifications. *Geoderma*, 133: 138-149.
- Neave, M. and S. Rayburg (2007), A field investigation into the effects of progressive rainfall-induced soil seal and crust development on runoff and erosion rates: The impact of surface cover, *Geomorphology*, 87(4), 378-390.
- Roering, J. J. (2004), Soil creep and convex-upward velocity profiles: Theoretical and experimental investigation of disturbance-driven sediment transport on hillslopes, *Earth Surface Processes and Landforms*, 29(13), 1597-1612.
- Roering, J. J. (2008), How well can hillslope evolution models "explain" topography? Simulating soil transport and production with high-resolution topographic data, *Geological Society of America Bulletin*, 120(9-10), 1248-1262.
- Saco, P. M., Willgoose, G.R., and Hancock, G. R., (2007) Eco-geomorphology of banded vegetation patterns in arid and semi-arid regions, *Hydrology and Earth System Sciences*, 11, 1717-1730.
- Sela, S., T. Svoray, and S. Assouline (2012), Soil water content variability at the hillslope scale: Impact of surface sealing, *Water Resources Research*, 48, W03522, doi: 10.1029/2011WR011297.
- Sommer, M., H. H. Gerke, and D. Deumlich (2008), Modelling soil landscape genesis - A "time split" approach for hummocky agricultural landscapes, *Geoderma*, 145(3-4), 480-493.
- Svoray, T., Karnieli A. 2011. Rainfall, topography, and primary production relationships in a semiarid ecosystem.

- Svoray, T., R. Shafran-Nathan, Z. Henkin, and A. Perevolotsky (2008), Spatially and temporally explicit modeling of conditions for primary production of annuals in dry environments, *Ecological Modelling*, 218(3-4), 339-353.
- Tarboton, D., G. (1997), A New Method for the Determination of Flow Directions and Contributing Areas in Grid Digital Elevation Models. *Water Resources Research*, 33(2), 309-319.
- Tarboton, D., G. (2010) Terrain Analysis Using Digital Elevation Models (TauDEM), Utah State University Logan, available at: <http://hydrology.neng.usu.edu/taudem>
- TOPOG (1997): <http://www-data.wron.csiro.au/topog/user/user.html>
- Tucker, G. E., and G. R. Hancock (2010), Modelling landscape evolution, *Earth Surface Processes and Landforms*, 35(1), 28-50.
- Vaks, A., M. Bar-Matthews, A. Ayalon, B. Schilman, M. Gilmour, C. J. Hawkesworth, A. Frumkin, A. Kaufman, and A. Matthews (2003), Paleoclimate reconstruction based on the timing of speleothem growth and oxygen and carbon isotope composition in a cave located in the rain shadow in Israel, *Quaternary Research*, 59(2), 182-193.
- Vaks, A., M. Bar-Matthews, A. Ayalon, A. Matthews, A. Frumkin, U. Dayan, L. Halicz, A. Almogi-Labin, and B. Schilman (2006), Paleoclimate and location of the border between Mediterranean climate region and the Saharo-Arabian Desert as revealed by speleothems from the northern Negev Desert, Israel, *Earth and Planetary Science Letters*, 249(3-4), 384-399.
- van Andel, T. H., E. Zangger, and A. Demitrac (1990), Land use and soil erosion in prehistoric and historic Greece , *Journal of Field Archaeology*, 17(4), 379-396.
- Wells, T., Willgoose G. and G Hancock G (2008), Modelling weathering pathways and processes of the fragmentation of salt weathered quartz-chlorite schist, *Journal of Geophysical Research- Earth Surface*, 113, F01014.
- Willgoose, G. R., and Sharmeen, S., (2006), A One-dimensional model for simulating armouring and erosion on hillslopes: I. Model development and event-scale dynamics, *Earth Surface Processes and Landforms*, 31, 970-991.
- Yair, A., and A. Kossovsky (2002), Climate and surface properties: hydrological response of small and semi-arid watersheds, *Geomorphology*, 42(1-2), 43-57.
- Yoo, K., and S. M. Mudd (2008), Discrepancy between mineral residence time and soil age: Implications for the interpretation of chemical weathering rates, *Geology*, 36(1), 35-38.
- Zilberman, E. (1992), The late Pleistocene sequence of the northwestern Negev flood plains — a key to reconstructing the paleoclimate of southern Israel in the last glacial, *Isr. J. Earth-Sci.* 41, 155-167.

Table and Figure captions

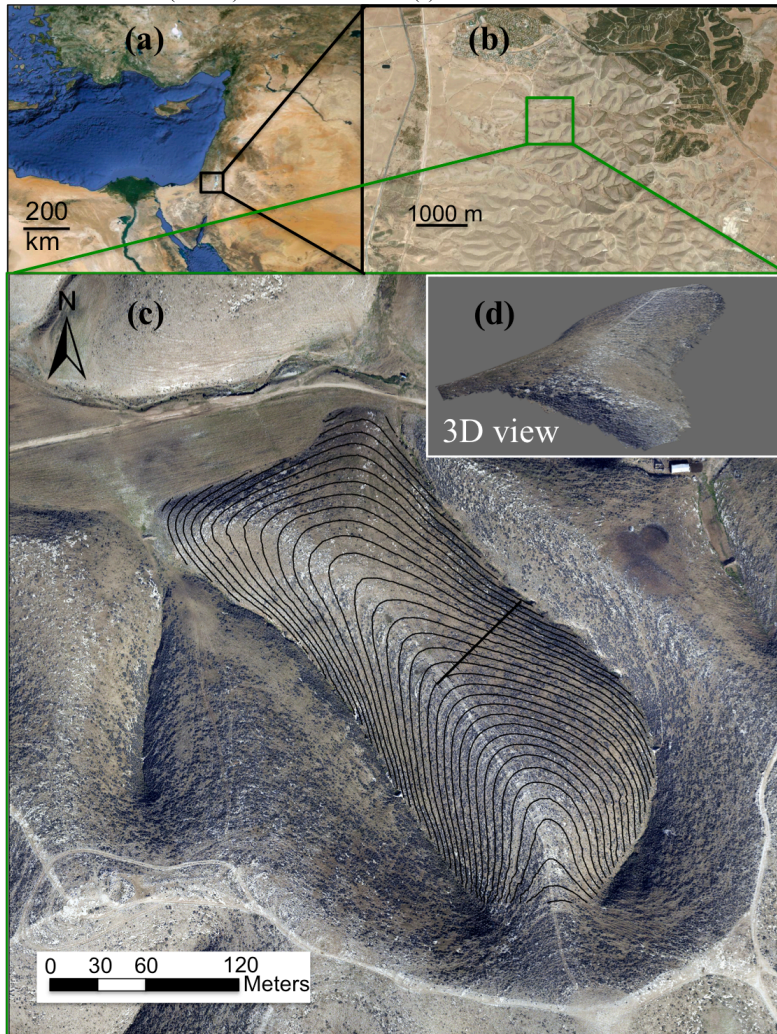
Table 1. Values of the parameters that are driven by the simulation scenario. P1, P2 and P3 are the three simulated periods (80-12, 12-8 and 8-0 kyr BP respectively; Figure 3) and S1, S2 and S3 are the three simulation (Fluvial, Diffusive and Combined respectively).

	<i>i</i> : Erodibility, e (unitless; Eq. 1)	<i>ii</i> : Runoff, Q (m^3/y ; Eq. 2)	<i>iii</i> : Aeolian deposition, K_a (mm/y; Eq. 5)	<i>iv</i> : Diffusive rate, D_o (mm/y; Eq. 3-4)
P1	S1: 0.0001 S2: 0.0 S3: 0.0001	S1: 0.0017 S2: 0.0 S3: 0.00066	S1: 0.1 S2: 0.1 S3: 0.1	S1: 0.0 S2: 21.5 S3: 12.0
P2	S1: 0.0002 S2: 0.0 S3: 0.0002	S1: 0.0034 S2: 0.0 S3: 0.00132	S1: 0.05 S2: 0.05 S3: 0.05	S1: 0.0 S2: 21.5 S3: 12.0
P3	S1: 0.001 S2: 0.0 S3: 0.001	S1: 0.017 S2: 0.0 S3: 0.0066	S1: 0.01 S2: 0.01 S3: 0.01	S1: 0.0 S2: 10.75 S3: 6.0

Sagy Cohen 11/21/2016 11:20 AM

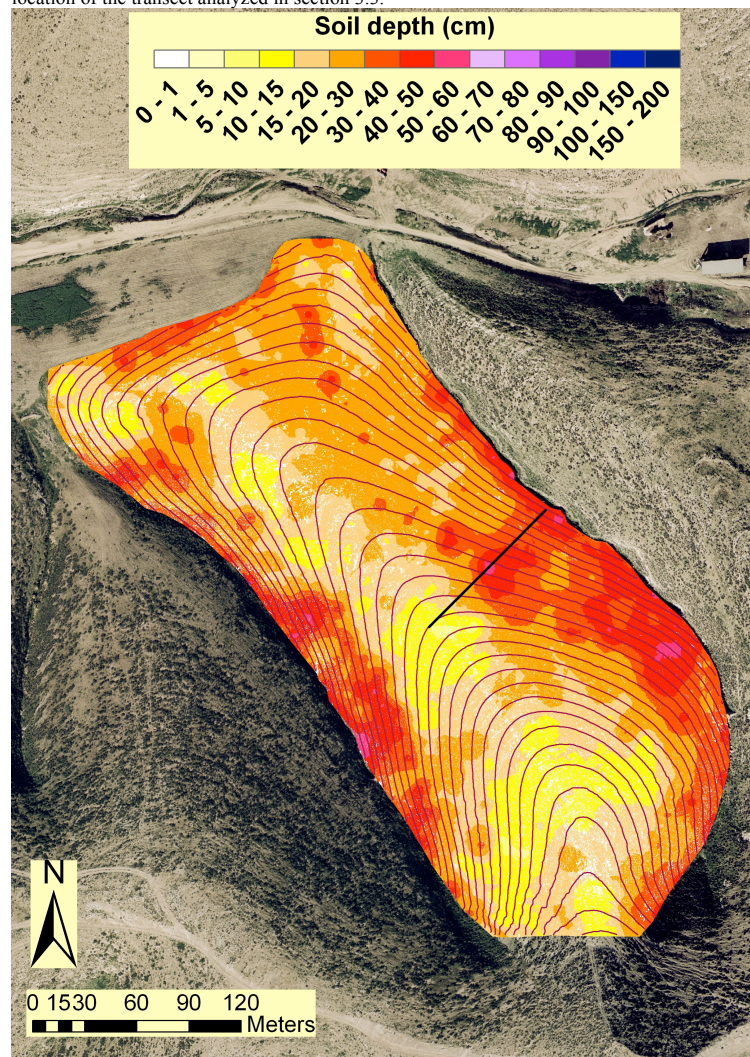
Deleted: D_s

Figure 1. The study region and site. The Long Term Ecological Research, LTER, in southern Israel, is uniquely situated at a margin between Mediterranean climatic regime to the north and arid climate to the south (a). The study site is located on a Loess belt (b) deposited during the late-Pleistocene and early-Holocene. Hillslopes in this region are today mostly depleted of their Loess cover (c and d). The contour lines in (c) are at 2 m intervals.



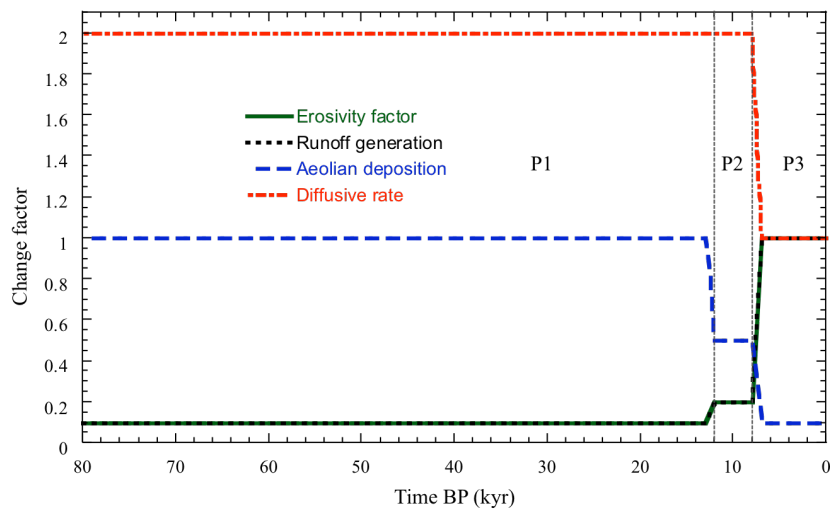
5

Figure 2. Soil depth at the Lehavim LTER site, measured in 350 locations and interpolated using Kriging. Pixels classified as rock from a 10 cm² orthophoto were assigned zero depth. The contour lines are at 2 m intervals and the thick black line is the location of the transect analyzed in section 3.3.



5

Figure 3. The simulation scenario. Describe the temporal changes in four model parameters as a function of climatic and anthropogenic drivers. The Erosion factor is overlapping with the Runoff generation line.



5

Figure 4. Soil depth maps produced by the Fluvial only simulation (S1) at 3.2 kyr time intervals in the last 18 of 80 kyr simulated; (a) 18 kyr BP (b) 12.8 kyr BP (end of P1); (c) 9.6 kyr BP; (d) 6.4 kyr BP (end of P2); (e) 3.2 kyr BP; and (f) 0 kyr BP (final/modern- end of P3). The contour lines represent 2 m change in topography.

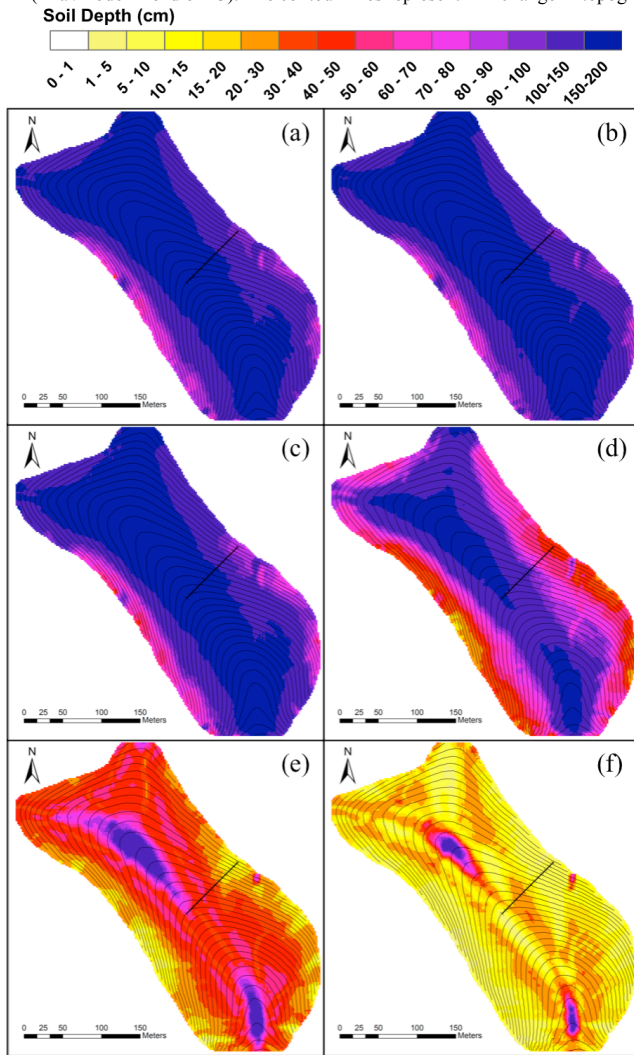


Figure 5. Soil depth maps produced by the Diffusive only simulation (S2) at 3.2 kyr time intervals in the last 18 of 80 kyr simulated: (a) 18 kyr BP (b) 12.8 kyr BP (end of P1); (c) 9.6 kyr BP; (d) 6.4 kyr BP (end of P2); (e) 3.2 kyr BP; and (f) 0 kyr BP (final/modern- end of P3). The contour lines represent 2 m change in topography.

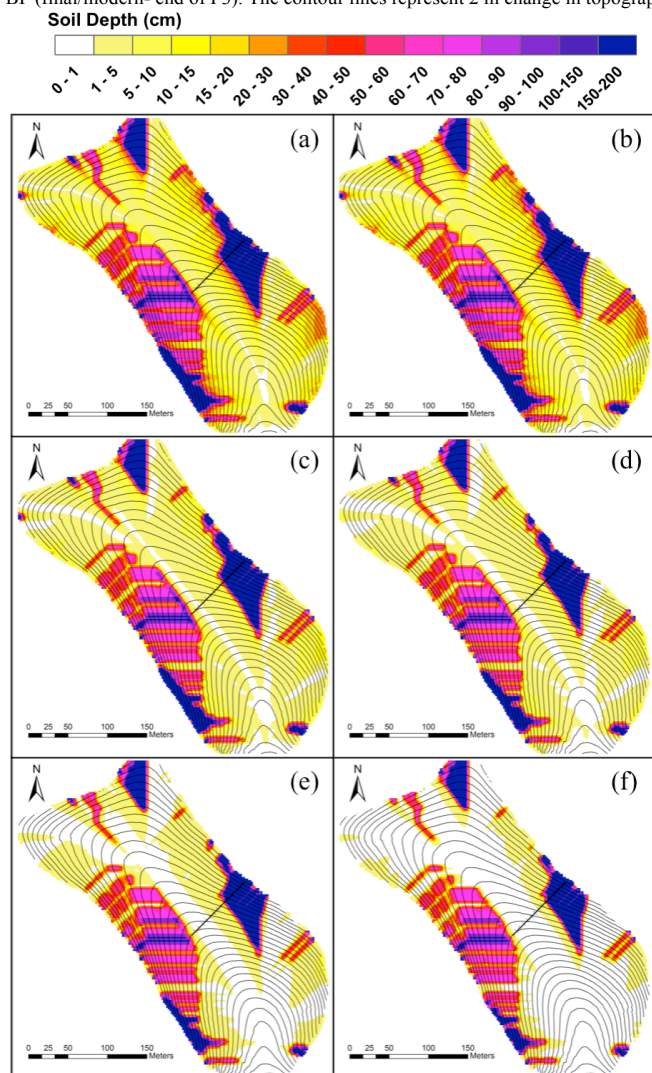


Figure 6. Soil depth maps produced by the Combined simulation (S3) at 3.2 kyr time intervals in the last 18 of 80 kyr simulated: (a) 18 kyr BP (b) 12.8 kyr BP (end of P1); (c) 9.6 kyr BP; (d) 6.4 kyr BP (end of P2); (e) 3.2 kyr BP; and (f) 0 kyr BP (final/modern- end of P3). The contour lines represent 2 m change in topography.

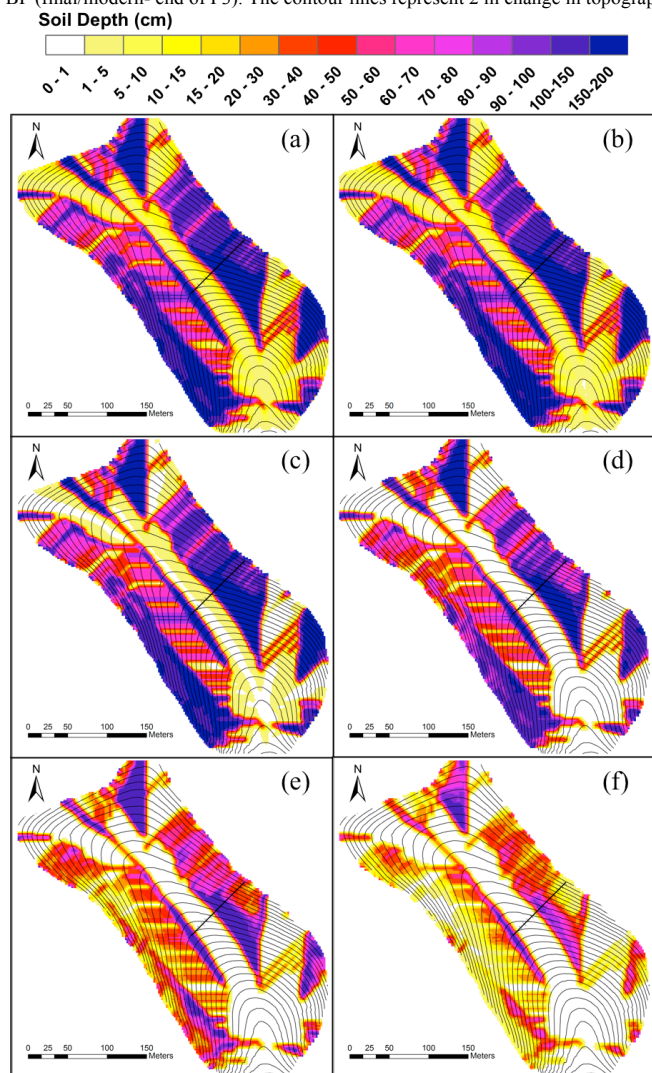
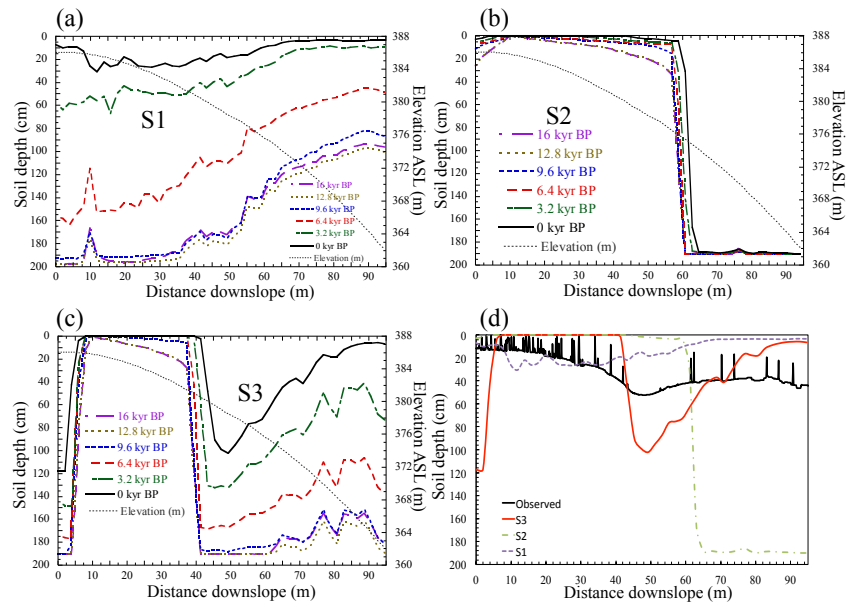


Figure 7. Soil depth across a transect (Figure 1c) on the northeastern facing hillslope at 6 time intervals (corresponding to soil maps in Figures 4-6): (a) the Fluvial only simulation (S1), (b) the Diffusive only simulation (S2), (c) the Combined simulation (S3), and (d) measured soil depth (Figure 2).



5